

On the role of athermal electrons in non-linear photoemission from Ag(100)

C. Giannetti^{1,a}, G. Ferrini², S. Pagliara², G. Galimberti², F. Banfi², E. Pedersoli², and F. Parmigiani³

¹ Dipartimento di Matematica e Fisica, Università Cattolica, 25121 Brescia, Italy
and

Sincrotrone Trieste, 34012 Basovizza, Trieste, Italy

² Dipartimento di Matematica e Fisica, Università Cattolica, 25121 Brescia, Italy

³ Dipartimento di Fisica, Università degli Studi di Trieste, and Sincrotrone Trieste, 34012 Basovizza, Trieste, Italy

Received 4 November 2005 / Received in final form 21 June 2006

Published online 22 August 2006 – © EDP Sciences, Società Italiana di Fisica, Springer-Verlag 2006

Abstract. The non-linear photoelectron spectra obtained by short laser pulses from a Ag(100) surface show a high-energy electron emission due to an athermal electron distribution created by the laser pulse. By comparing the photoemission at normal and non-normal emission geometry it is possible to evidence the independence of the hot electron photoemission on the parallel momentum and on different final-state configurations. A photoemission correlation measurement evidences that non-photoelectric effects, as tunneling or thermally assisted photoemission, do not contribute to the electron yield. Various theoretical models are discussed on the basis of the present data.

PACS. 79.60.-i Photoemission and photoelectron spectra – 73.50.Gr Charge carriers: generation, recombination, lifetime, trapping, mean free paths – 78.47.+p Time-resolved optical spectroscopies and other ultrafast optical measurements in condensed matter

The dynamics of the non-equilibrium electron distribution in solids, induced by excitation with ultrashort laser pulses, has been widely investigated in the last decade. Time-resolved two-photon photoemission (2PPE) has contributed to the detailed investigation of the non-equilibrium electron dynamics and has been crucial for the understanding of the role played by electron-electron and electron-phonon scattering in the relaxation processes [1–3]. In addition, the femtosecond excitation of a non-equilibrium electron distribution is a powerful tool to study the problem of charge transfer between a metallic substrate and adsorbate or polar molecules overlayers, a relevant topic in modern femtochemistry [4].

Recently, higher-order multiphoton photoemission processes has been recognized as an important extension of 2PPE technique, increasing the energy range of the unoccupied states that can be studied and providing information on the photoexcitation mechanisms [5–7]. Few studies have investigated the influence of band structure on this kind of processes, especially when above-threshold photoemission is involved, a process in which the last multiphoton electron transition is entirely above the vacuum level. The role played by the non-equilibrium electron distribution in the non-linear photoemission process has not been entirely clarified and the role of the intermediate states, especially in cases where no electron bulk band

states are available, e.g. when the intermediate state fall in a band gap, is not well understood and is a subject of discussion [8].

In this report, we focus on the nonlinear photoemission of electrons excited so that the intermediate states are within the extended band gap region along the (100) direction of Ag. The photoemission spectra are obtained by exciting the electrons by short laser pulses in a regime where the equilibrium distribution of the bulk electrons is negligibly perturbed and a small population of excited electrons, whose equilibrium electron temperature is not defined, is far from equilibrium. By comparing the photoemission at normal and non-normal emission geometry it is possible to evidence the independence of the hot electron photoemission on the parallel momentum and from different final and intermediate states configurations. A photoemission correlation measurement evidences that nonphotoelectric effects, as tunneling or thermally assisted photoemission, do not contribute to the electron yield. These experimental evidences can be rationalized in terms of a non-thermal electron population subject to interactions such as phonon scattering [9], inverse bremsstrahlung processes [10] or transient exciton formation [11] that quench the dependence of photoelectric emission on electron momentum and band structure.

The photoemission experiments were carried out in a ultrahigh vacuum system (pressure $\leq 5 \times 10^{-10}$ mbar) at

^a e-mail: c.giannetti@dmf.unicatt.it

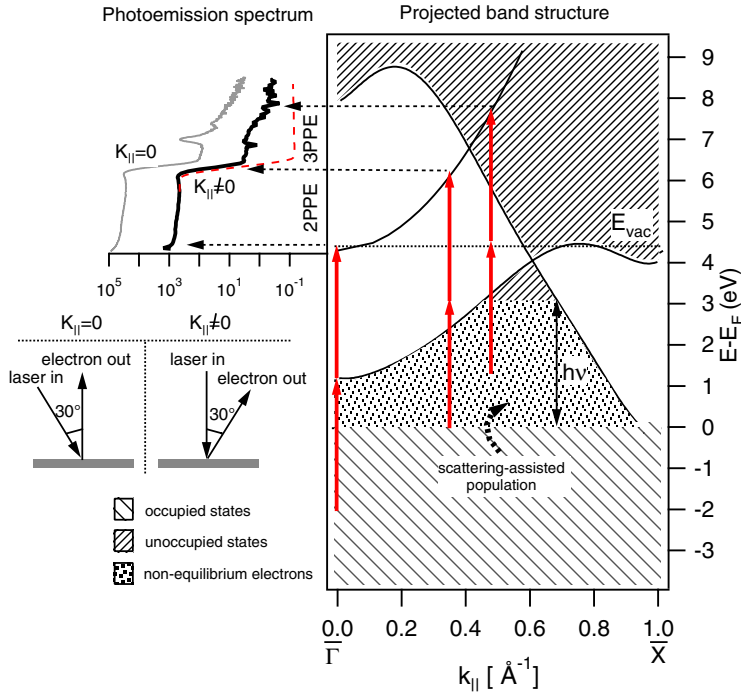


Fig. 1. Photoemission spectra measured at 30° emission angle (black line) and normal emission angle (gray line). The red dashed line simulates the step-like structure expected in the case of coherent photoemission. The projected band structure along the $\bar{\Gamma}\bar{X}$ direction of Ag(100) surface Brillouin zone is shown (taken from Ref. [21]). A measured work-function of 4.3 eV is reported.

room temperature (300 K). The sample was an Ag crystal cut along the (100) direction within 0.5° approximation. A clean and ordered surface was obtained by standard sputtering and annealing procedures. The light pulses ($\hbar\omega = 3.14$ eV, timewidth 130 fs, p -polarized) were obtained by doubling the output of an amplified Ti:Sapphire laser system. The size of the spot, about $300 \times 300 \mu\text{m}^2$, was chosen to have a high count rate minimizing space-charge effects in the photoemission spectra. The kinetic energy of the photoemitted electrons was measured by a time of flight (ToF) spectrometer. The total energy resolution of the experimental set-up (laser linewidth plus detector resolution) is 35 meV at a kinetic energy of 2 eV.

When a metal sample is excited by short light pulses with a photon energy smaller than the work-function, different nonlinear photoelectric processes can contribute to the photoemission spectrum. The typical appearance of a nonlinear photoemission spectrum is reported in Figure 1 (black line). The final state energy of the electrons is measured from the Fermi energy E_F , the emission angle is 30° at normal light incidence. The 2PPE and 3PPE spectral regions are indicated. A high-energy electron tail that departs from the 2-photon Fermi edge is related to the photoemission from a non-equilibrium electron distribution excited in the empty bulk states. In this case the photoemission mechanism is a 3PPE process [7, 12].

A non-normal emission geometry implies that different parallel momenta (k_{\parallel}) are associated with electrons ejected with different kinetic energies E_{kin} . The relationship between k_{\parallel} and the kinetic energy at $\vartheta = 30^\circ$ emission is:

$$k_{\parallel} (\text{\AA}^{-1}) = \frac{\sqrt{2m_e E_{kin}}}{\hbar} \sin \vartheta = 0.256 \sqrt{E_{kin} (\text{eV})} \quad (1)$$

where m_e is the free electron mass. In the projected band structure scheme, reported in Figure 1, the dependence of the measured external kinetic energy on the parallel momentum is shown. The 3PPE kinetic energy region spans a k_{\parallel} interval between 0.3 – 0.5 \AA^{-1} . As can be seen from the band structure scheme reported, the spectra spans a parallel momentum interval where the final states cross the border between the gap and the empty bands. The lack of discontinuities in the photoemission spectrum near the empty-bands crossing suggests a minor role played by the final states in the 3PPE above-threshold process.

The structure of spectra taken at normal emission ($k_{\parallel} = 0$), reported in gray in the figure, do not differ from non-normal emission spectra, except for the presence of image potential states (IPS), that can not be photoemitted at large emission angles. The excited non-equilibrium electrons populate IPS by scattering assisted indirect processes, inducing an effective mass variation and electric dipole selection rules violation [6]. The similar behavior of the 3PPE regions at different k_{\parallel} is the signature of the independence of this photoemission process on the availability of intermediate states.

According to the recent literature, three different processes contribute to multiphoton transitions in a nonlinear photoemission process [13, 14]. *Coherent* transitions, when the intermediate state is a virtual state. *Direct* transitions, when the intermediate state is a real state and there is no change of the electron momentum parallel to the surface sample (also referred to as resonant transitions). *Indirect* transitions, when the electron momentum parallel to the sample surface is not conserved during the transition from the initial to the final state. The high-kinetic electron tail detected in the reported spectra can not be explained by a coherent photoemission because the

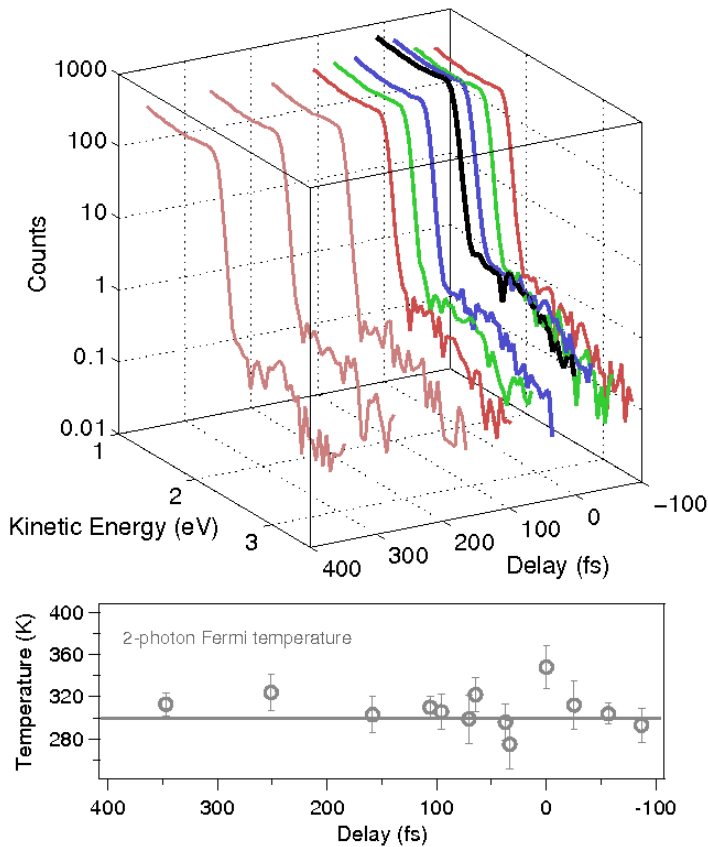


Fig. 2. The photoemission spectra are plotted versus the delay time between pump and probe pulses. The pump and probe measurements are carried out at normal incidence and at an angle of 30° between the detector and the normal to the sample surface. Some spectra are omitted for graphical reasons. In the inset the 2-photon Fermi edge temperature associated to each spectrum is reported. The temperature spike seen at 0-delay is attributed to a small space-charge deformation since this timescale is too short for any energy exchange between the electron system and the phonon gas.

expected step-like structure (see red dashed line in Fig. 1) of the spectrum is not reproduced by experiments. Moreover, direct resonant dipole transitions between two levels in the conduction band are not allowed in the dipole approximation. This follows from the energy and quasimomentum conservation [9].

A plausible mechanism to explain the high-energy electron tail is an *indirect* 3PPE process, mediated by scattering events which change the k_{\parallel} -momentum of the photoemitted electrons. In this picture the scattering mediated photon absorption creates a non-equilibrium electron population in the unoccupied bulk states at $k_{\parallel} \neq 0$, where available states extend up to the vacuum level. A scattering event is also responsible for the electron k_{\parallel} -momentum exchange necessary to the photoemission process, as shown in Figure 1. The scattering mediated absorption completely relaxes the selection rules and the dependence on k_{\parallel} , thus explaining the similarity between normal emission and non-normal emission spectra. This interpretation is consistent with two recent theoretical works that investigate the interaction of the laser field with the excited non-equilibrium conduction electrons in metals. Photon absorption is attributed to electron collisions with phonons [9] or to an inverse bremsstrahlung process [10].

Our findings can be explained also by the creation of transient excitonic states, through multi-photon absorption. It was speculated that the observed states in band gaps are caused by an attractive interaction between the

photoelectron and its localized hole in the d bands, due to the finite time it takes the valence band electrons to screen the photohole [15]. Successive theoretical models confirmed this possibility [11]. In this case the intermediate electron states are given by the transient excitonic levels created by the laser photohole production. We note that all the proposed models [9–11] are based on *ab initio* results, without invoking the so-called transport correction [8, 16].

To investigate the origin of the athermal part of the excited electrons, a photoemission autocorrelation is used, i.e. electron spectra are measured as a function of the delay between two *identical* pulses. Differently from a pump and probe experiments, where the electron population is excited (without photoemission) by the optical pump and emitted by the probe pulse, in photoemission autocorrelation both pulses produce a complete electronic spectrum. The correlation of identical pulses via the photoemitted nonlinear spectra gives information on the relaxation dynamics, the nonlinear order of the photoemission process, and gives indication on the dependence on non photoelectric effects, such as tunneling processes and thermally assisted photoemission [17].

In Figure 2 the spectra as a function of the delay between two collinear pulses are shown. Normal light incidence prevents artifacts due to different absorption coefficients from the cross polarized beams. It is important to note the difference of about 4 order of magnitude in the 2PPE and 3PPE yields. In order to obtain reasonable

electron statistics in the 3PPE region, the typical duration of each spectrum collection is several hours. As a consequence, fluctuations and drifts of the laser intensity result in a scattering of the non-linear photoemission intensity, which can not be totally compensated by renormalization to the mean incident power.

Previous pump and probe measurements [18,19] of the thermalization of the non-equilibrium electron population were performed on a polycrystalline metal film irradiated by femtosecond laser pulses, with an incident fluence larger than 1 GW/cm^2 . In this case, the absorption of the e.m. field energy resulted in a strong perturbation of the equilibrium electron distribution, with an electronic temperature increase up to 400 K. On the contrary, our measurements are carried out with a laser intensity of about one order of magnitude lower. For this reason the equilibrium electron distribution is weakly perturbed after the absorption of the laser pulse. The temperature increase of the 2PPE Fermi distribution in the time resolved spectra shown in Figure 2, due to energy exchange between the photoexcited electron population and the bulk-electrons, is at most few tens degrees. The 2-photon Fermi edge of the spectra at various delays is fitted with a Fermi-Dirac function convoluted with a Gaussian function, to take into account the apparatus resolution. The temperature increase of the equilibrium electron distribution, measured when the delay exceeded the laser pulse duration, is about 20 K. The calculated Fermi temperature using the two-temperature model is $\sim 345 \text{ K}$ after a single laser pulse, a value compatible with that measured in this work.

In Figure 3 the electron yield from the 2PPE and 3PPE spectral regions is shown as a function of the delay. To measure the nonlinearity of the photoemission process in each spectral region, the electron yield vs. laser fluence (I) is reported in the inset. The electron yield in the Fermi edge 2PPE region ($1.66 \leq E_{kin} \leq 1.88$) has a I^2 power law dependence on laser fluence, as expected for a 2PPE process. The electron yield in the 3PPE region ($2.18 \leq E_{kin} \leq 3.5$) has a I^3 dependence on fluence, in agreement with the result reported in reference [12]. Since each region has a different photoemission nonlinearity, to compensate for laser intensity drifts, we normalized the electron yield using the mean laser intensity (I_0) to the corresponding power law dependence (I_0^2 for 2PPE and I_0^3 for the 3PPE regions).

The autocorrelation of the photoemission yield from each region shows an instantaneous response to the laser excitation on the temporal scale of the pulse timewidth. This result confirms that, within the pulse duration, the laser electric field coexists with a non-equilibrium electron gas which is thermalizing through electron-electron scattering on the same timescale. An estimate of the scattering rate τ of the electron gas averaged over the 3PPE region, using the Fermi liquid theory [22], gives a mean scattering time of $\langle \tau \rangle \simeq 23 \text{ fs}$. This value is compatible with a decay time of the non-equilibrium population shorter than the 130 fs pulse timewidth.

In the 2PPE spectral region the ratio between the measured intensity at $\Delta t = 0$ ($I_0 \propto |E_{pump} + E_{probe}|^2 =$

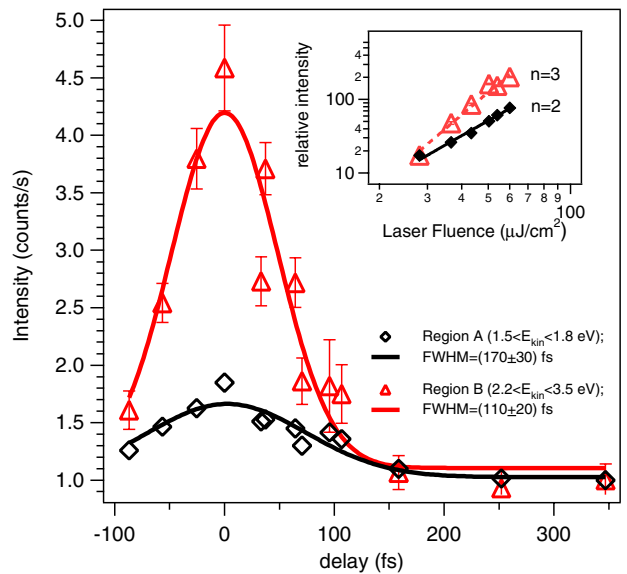


Fig. 3. The photoemission integrated intensities are plotted versus the delay time between the pump and the probe pulses. The pump and probe measurements are carried out at normal incidence and at an angle of 30° between the detector and the normal to the sample surface. In the inset the integrated intensities for the Fermi (diamonds) and high-energy electron (triangles) regions are plotted versus the incident laser fluence. In order to estimate the non linearity order (n), the data are fitted with a power function.

$4E_{pump}^2$) and the background intensity, measured at $\Delta t = 300 \text{ fs}$ ($I_\infty \propto |E_{pump}|^2 + |E_{probe}|^2 = 2E_{pump}^2$) is 1.85, compatible with the value 2 for a second order process. In the 3PPE spectral region the I_0/I_∞ ratio is 4.6, compatible with the value 4 for a third order photoemission process.

The close correspondence between the non-linearities measured by laser electron vs. fluence yield and autocorrelation peak to background contrast ratio (PBCR) is an indication that temperature assisted processes are negligible. In fact, a thermally assisted photoemission could result in a dependence of the electron yield on electron temperature. Since the time scale of electron temperature relaxation is one picosecond, this could result in a yield increase on the wings of the autocorrelation and a modification of the PBCR for delays smaller than the electron-lattice relaxation constant [17,20]. Ruling out thermally assisted processes is important in view of the proposed models to explain short pulse photoemission: both scattering assisted photoemission and transient exciton formation are extremely rapid processes, on the scale of few tens of femtoseconds, that are decoupled from the electron thermal bath.

The reported results confirms that the non-equilibrium electron population created by a laser pulse at very low laser intensities ($I \simeq 0.1 \text{ GW/cm}^2$) on Ag single crystal, perturbs in a negligible way the equilibrium bulk electron system, which behaves as a thermal bath. For this reason the recently reported variations of the properties of the indirectly populated IPS [6], such as a difference in the

effective mass, can not be attributed to a perturbation of the properties of the equilibrium electron distribution. The physical mechanism responsible for these variations, has to be found in the population mechanism or in the interaction of electrons in IPS with the non-equilibrium population.

In conclusion, the photoemission from the athermal electron gas is due to a pure photoelectric process where forbidden dipole transition in *sp* bands are allowed through phonon scattering or through intermediate transient state formation by excitonic mechanisms. The absence of thermal contribution is confirmed by photoemission autocorrelation measurements.

References

1. R. Haight, Surf. Sci. Reports **21**, 275 (1995)
2. P. Petek, S. Ogawa, Progr. Surf. Sci. **56**, 239 (1997)
3. P.M. Echenique, R. Berndt, E.V. Chulkov, T.H. Fauster, A. Goldmann, U. Hofer, Surf. Sci. Rep. **52**, 219 (2004)
4. A.D. Miller, I. Bezel, K.J. Gaffney, S. Garrett-Roe, S.H. Liu, P. Szymanski, C.B. Harris, Science **297**, 1163 (2002)
5. G.P. Banfi, G. Ferrini, M. Peloi, F. Parmigiani, Phys. Rev. B **67**, 035428 (2003)
6. G. Ferrini, C. Giannetti, G. Galimberti, S. Pagliara, D. Fausti, F. Banfi, F. Parmigiani, Phys. Rev. Lett. **92**, 256802 (2004)
7. F. Bisio, M. Nývlt, J. Franta, H. Petek, J. Kirschner, Phys. Rev. Lett. **96**, 087601 (2006)
8. W. Eckart, W.-D. Schöne, R. Keiling, Appl. Phys. A **71**, 529 (2000)
9. A.V. Lugovskoy, I. Bray, Phys. Rev. B **60**, 3279 (1999)
10. B. Rethfeld, A. Kaiser, M. Vicanek, G. Simon, Phys. Rev. B **65**, 214303 (2002)
11. W.-D. Schöne, W. Eckart, Phys. Rev. B **65**, 113112 (2002)
12. F. Banfi, C. Giannetti, G. Ferrini, G. Galimberti, S. Pagliara, D. Fausti, F. Parmigiani, Phys. Rev. Lett. **94**, 037601 (2005)
13. S. Ogawa, H. Nagano, H. Petek, Phys. Rev. B **55**, 10869 (1997)
14. T. Hertel, E. Knoesel, M. Wolf, G. Ertl, Phys. Rev. Lett. **76**, 535 (1996)
15. J. Cao, Y. Gao, R.J. Miller, H.E. Elsayed-Ali, D.A. Mantell, Phys. Rev. B **56**, 1099 (1997)
16. E. Knoesel, A. Hotzel, M. Wolf, Phys. Rev. B **57**, 12812 (1998)
17. J.G. Fujimoto, J.M. Liu, E.P. Ippen, N. Bloembergen, Phys. Rev. Lett. **53**, 1387 (1984)
18. W.S. Fann, R. Storz, H.W.K. Tom, J. Bokor, Phys. Rev. Lett. **68**, 2834 (1992)
19. W.S. Fann, R. Storz, H.W.K. Tom, J. Bokor, Phys. Rev. B **46**, 13592 (1992)
20. A. Bartoli, G. Ferrini, L. Fini, G. Gabetta, F. Parmigiani, F.T. Arecchi, Phys. Rev. B **56**, 1107 (1997)
21. Z. Li, S. Gao, Phys. Rev. B **50**, 15394 (1994)
22. D. Pines, P. Nozieres, *The Theory of Quantum Liquids* (Benjamin, New York, 1969)